Remote Sensing of Environment 152 (2014) 603–613

Contents lists available at ScienceDirect

Remote Sensing of Environment

journal homepage: www.elsevier.com/locate/rse

The HelioMont method for assessing solar irradiance over complex terrain: Validation and improvements

M. Castelli [a,c,*], R. Stöckli [b], D. Zardi [a], A. Tetzlaff [c], J.E. Wagner [c], G. Belluardo [d], M. Zebisch [c], M. Petitta [e]

[a] Atmospheric Physics Group, Department of Civil, Environmental and Mechanical Engineering, University of Trento, via Mesiano 77, 38123 Trento, Italy
[b] Federal Office of Meteorology and Climatology MeteoSwiss, Krähbühlstrasse 58, 8044 Zürich, Switzerland
[c] Institute for Applied Remote Sensing, European Academy of Bolzano, via Druso 1, 39100 Bolzano, Italy
[d] Institute for Renewable Energy, European Academy of Bolzano, Via Luis-Zuegg 11, 39100 Bolzano, Italy
[e] UPRSE, ENEA Casaccia, Via Anguillarese 301, 00123 Roma, Italy

ARTICLE INFO

Article history:
Received 15 May 2013
Received in revised form 19 June 2014
Accepted 20 July 2014
Available online 13 August 2014

Keywords:
Solar surface irradiance
Diffuse radiation
Aerosols
Radiative transfer modeling
Remote sensing

ABSTRACT

This study evaluates the suitability of the method HelioMont, developed by MeteoSwiss, for estimating solar radiation from geostationary satellite data over the Alpine region. The algorithm accounts for the influence of topography, clouds, snow cover and the atmosphere on incoming solar radiation. The main error sources are investigated for both direct and diffuse solar radiation components by comparison with ground-based measurement taken at three sites, namely Bolzano (IT), Davos (CH) and Payerne (CH), encompassing different topographic conditions. The comparison shows that the method provides high accuracy of the yearly cycle: the Mean Absolute Bias (MAB) is below 5 W m^{-2} at the lowland station Payerne and below 12 W m^{-2} at the other two mountainous stations for the monthly averages of global and diffuse radiation. For diffuse radiation the MAB is in the range 11–15 W m^{-2} for daily means and 34–40 W m^{-2} for hourly means. It is found that the largest errors in diffuse and direct radiation components on shorter time scales occur during summer and for cloud-free days. In both Bolzano and Davos the errors for daily-mean diffuse radiation can exceed 50 W m^{-2} under such conditions. As HelioMont uses monthly climatological values of atmospheric aerosol characteristics, the effects of this approximation are investigated by simulating clear-sky solar radiation with the radiative transfer model (RTM) libRadtran using instantaneous aerosol measurements. Both ground-based and satellite-based data on aerosol optical properties and water vapor column amount are evaluated. When using daily atmospheric input the estimation of the hourly averages improves significantly and the mean error is reduced to 10–20 W m^{-2}. These results suggest the need for a more detailed characterization of the local-scale clear-sky atmospheric conditions for modeling solar radiation on daily and hourly time scales.

1. Introduction

An accurate estimation of solar radiation at the Earth surface is a key requirement for climate monitoring and for hydrological and biological applications. Indeed, various biophysical and biochemical processes on the Earth surface are driven by solar radiation, with feedbacks to the rest of the climate system (Bonan, 2002). These include the diurnal development of the atmospheric boundary layer in response to diurnal exchanges of energy, mass and momentum between the atmosphere and the Earth surface and thermally driven flows over complex terrain (Serafin & Zardi, 2010a,b, 2011). Solar radiation is also a main driver for plant photosynthesis and evapotranspiration (Sellers et al., 1997). The spatial and temporal quantification of solar radiation is required for planning and modeling purposes in various areas, such as agriculture, forestry and oceanography. In particular the role of radiation on the peculiar energy budgets occurring in urban areas and the related effects, such as the urban heat island, have been the subject of recent investigations (Giovannini, Zardi, & de Franceschi, 2011, 2013; Giovannini, Zardi, de Franceschi, & Chen, 2014). Models for quantifying evapotranspiration, which is a major input in soil water balance analyses, also use solar radiation as input, together with other meteorological variables and soil properties (Carrer et al., 2012; Sellers et al., 1996). The assessment of solar energy is also essential in applications converting solar radiation into electricity, such as photovoltaic plants and concentrated solar power systems. One main limitation of the competitiveness of photovoltaic and concentrated solar power systems with other sources of energy is the high cost of the active solar materials. Besides the current research on innovative and more economic semiconductor materials (Barber et al., 2011), another way towards improving the efficiency of solar power is a more accurate estimation of solar radiation at the project development stage. In fact, the evaluation of the direct and diffuse

* Corresponding author at: Via Druso 1, 39100 Bolzano, Italy. Tel.: +39 0471 055 381.
E-mail address: mariapina.castelli@eurac.edu (M. Castelli).

http://dx.doi.org/10.1016/j.rse.2014.07.018

components of solar radiation is essential for supporting the choice of the best available technology, i.e. the one that most effectively exploits the radiation available in a target area. Accordingly, the present work aims at investigating the accuracy of the latest modeling techniques for estimating solar radiation at the Earth surface from satellite data in the Alps.

One way for assessing solar irradiance is the analysis of data from ground-based radiometers. The expected error in irradiance calculation is due to the difference between operation and calibration conditions. For high quality and well maintained instruments, such as those used in this study, the World Meteorological Organization (WMO) guidelines admit maximum errors in the hourly radiation totals of 3% (World Meteorological Organization, 2008). Unfortunately in most cases ground networks of radiometers do not cover sufficiently the area of interest. For example in the province of Bolzano, in the Italian Alps, which is the area of major interest for the project which motivated the present work, all measurement stations are located more than 5 km from each other, whereas the spatial autocorrelation of solar radiation is generally less than 1 km (Dubayah, 1992; Dubayah & Paul, 1995). In addition conventional weather stations usually include global radiometers and only few of them are equipped with radiometers measuring either the diffuse or direct component of radiation. Considering the limitations of the network of ground-based instruments, especially over complex terrain, it is necessary to consider other ways for addressing the problem of estimating surface radiation.

Radiative transfer models (RTMs), simulating the incoming solar radiation through all its interactions with the atmosphere and the Earth surface, can for instance be used. These models can simulate the absorbing and scattering effects of atmospheric gases and particles, clouds or surface reflections and shadows (Kato, Ackerman, Mather, & Clothiaux, 1999; Liou, 2002; Stamnes et al., 1988; Stamnes, Tsay, Wiscombe, & Laszlo, 2000). The disadvantage of using RTMs is that accurate calculations are time consuming, thus not convenient for application to large areas. RTMs also require a substantial amount of information concerning rapidly changing atmospheric conditions, such as clouds and aerosol properties. However, the radiative forcing of clouds and, to a certain degree, also aerosol properties can be retrieved from satellite observations. In particular, geostationary satellite data offer a high frequency of observation, thus allowing to observe the daily variability of cloud cover. The main drawbacks of using geostationary satellite data are their coarse spatial resolution and large view angles for higher latitudes. These limitations are particularly severe in mountainous regions, where the altitude varies sharply and affects not only surface related parameters, but also the state of the atmosphere. Furthermore satellite radiometers measure visible radiation reflected by the Earth's atmosphere, thus the retrieval of downward radiation at the Earth surface is not trivial, and requires the modeling of the physical interactions between radiation and aerosols, gases and clouds.

The main effort for retrieving solar radiation at the Earth surface from meteorological satellite data was done in the late eighties (Cano et al., 1986) for Meteosat radiometers data. The idea was to correlate the observed reflectivity of each pixel with its cloudiness. First a reference surface albedo map was evaluated statistically. Then a cloud index n, a surrogate for the cloud radiative forcing of a pixel, was calculated. It was defined as the measured albedo, ρ, normalized to the difference between its maximum (ρ_{max}), observed under overcast sky conditions, and minimum (ρ_{min}), corresponding to a reference albedo calculated for cloud-free conditions:

$$n = \frac{\rho - \rho_{min}}{\rho_{max} - \rho_{min}}. \quad (1)$$

A linear proportionality was assumed between irradiance at the top of the atmosphere and global radiation at the Earth surface, the coefficient of proportionality being the so called atmospheric transmission factor, K. The factor K was calculated as an empirical function of n by using pyranometric measurements as test dataset (Fontoynont et al., 1997, 1998; Hammer et al., 2003). The original radiation retrieval method was called HELIOSAT and was proposed in many formulations following different sensor generations (Beyer, Costanzo, & Heinemann, 1996; Hammer et al., 2003; Rigollier, Lefèvre, & Wald, 2004), mainly changing the clear-sky model used for calculating cloud-free irradiance and the relation between n and K.

One version of HELIOSAT which analyzes the peculiar conditions of mountainous areas was proposed by Dürr and Zelenka (2009) specifically for the Alps. This model includes snow detection, pixel georeferencing, satellite view angle distortion fixing, and terrain shading calculation. Despite its comprehensiveness, this algorithm approximates the transmissivity of the atmosphere only through monthly climatological values of the Linke turbidity coefficient (Remund, Wald, Lefvre, Ranchin, & Page, 2003). The turbidity is included in the empirical clear-sky model of Kasten, Dehne, Behr, and Bergholter (1984), and does not affect the procedure used to calculate the diffuse radiation fraction. At the same time a new clear-sky model for HELIOSAT was proposed: the algorithm SOLIS (Müller et al., 2004). The latter is based on RTM simulations of clear-sky irradiance. Later on SOLIS was modified introducing the computationally efficient *look up tables* approach, which means that RTM runs were performed for discrete values of the atmospheric parameters, and then an interpolation was performed in dependence of atmospheric input data. This model was called MAGIC (Müller et al., 2009). Radiation values obtained with the *look up tables* approach differ from the exact RTM solutions by no more than 1–2 W m^{-2}. Recently MeteoSwiss has coupled the MAGIC clear-sky model with a new processing scheme for the all-sky retrieval of solar radiation at surface. This new algorithm, called HelioMont, is comprehensively documented in Stöckli (2013) and briefly described in the next section.

HELIOSAT versions including the *look up tables* approach were variously validated and results are reported in many papers. For example in Ineichen et al. (2009) the hourly averages of global irradiance were validated against 8 European stations during 4 months. An overall Root Mean Square Error (RMSE) between 80 and 100 W m^{-2} and Mean Bias Deviation (MBD) between −15 and 20 W m^{-2} were found. Clear-sky and overcast conditions were also considered separately, finding an underestimation in the first case and an overestimation in the second one. The underestimation in clear-sky cases was also correlated to an overestimation of the Aerosol Optical Thickness (AOT) used for the interpolation from the look up tables. Furthermore, Journée and Bertrand (2010) validated global irradiance at 13 sites in Belgium. The 10 minute averages of ground measurements were compared to the satellite estimations derived from the corresponding instantaneous observations, with a resolution of 1 h. Mean Absolute Bias (MAB) larger than 60 W m^{-2} and MBD between −18 and 8 W m^{-2} were observed. An underestimation in clear-sky conditions has been noticed also in the last mentioned paper. Some validation results can also be found in Betcke et al. (2006). However, to the best of our knowledge, no detailed analysis of the diffuse and direct irradiance components calculated with the *look up tables* approach has been done so far. Moreover no validation studies have been performed with satellite-derived solar irradiance over complex terrain, with the exception of Dürr et al. (2010).

This paper aims at assessing the reliability of the HelioMont method for retrieving irradiance from Meteosat Second Generation (MSG) satellite data at three specific measurement locations in the Alps encompassing different topographic conditions. In particular the realism of the algorithm in estimating the direct and diffuse components of solar radiation is investigated with respect to atmospheric input data, such as aerosol properties.

The structure of this paper is as follows: Section 2 describes the algorithm HelioMont and gives the technical details of the ground measurements used for the validation; Section 3 presents the results of the validation on different time scales and under different sky conditions; Section 4 shows the results of RTM simulations of solar radiation to emphasize the role of aerosols; in the last section the conclusions

derived from the outcome of the present analysis are summarized and discussed, and possible applications of the results are proposed.

2. Data and method

The present study validates shortwave solar radiation at the Earth surface, derived by MeteoSwiss from MSG data, against surface based point measurements. We investigated separately global irradiance (SIS, Surface Incoming Shortwave Radiation) and its diffuse (SISDIF, Surface Incoming Shortwave Radiation — Diffuse component) and direct normal (SISDNI, Surface Incoming Shortwave Radiation — Direct Normal Irradiance) components, since they can be used in different applications and their relative amount influences the efficiency of their exploitation.

The statistical parameters adopted here to compare the irradiance components are the Mean Bias Deviation (MBD), the Mean Absolute Bias (MAB), the Root Mean Square Error (RMSE), and the R squared correlation coefficient of the linear regression between satellite estimate and ground-based measurements (R^2). All these parameters are calculated according to the formulation of Wilks (2011), i.e.:

$$MBD = \frac{1}{n}\sum_{i=1}^{n}(S_i - G_i) \tag{2}$$

$$MAB = \frac{1}{n}\sum_{i=1}^{n}|S_i - G_i| \tag{3}$$

$$RMSE = \sqrt{\frac{1}{n}\sum_{i=1}^{n}(S_i - G_i)^2} \tag{4}$$

where S_i is the modeled variable and G_i is the observed variable averaged in the ith time interval. Since the processing of MSG data is limited to slots corresponding to sun elevation angles above 3°, we filled the few missing MSG data using the relation between all-sky and cloud-free irradiance, whose ratio is generally referred to as clear-sky index (k). We calculated the daily average clear-sky index (k_d), both for global and direct irradiance, as the ratio between the daily mean irradiance and the daily mean clear-sky radiation:

$$k_d = \frac{SIS_d}{SIS_{d,\ cloud-free}}. \tag{5}$$

Afterwards we replaced instantaneous missing data with the product of k_d and the instantaneous clear-sky irradiance, which is modeled with the MAGIC approach:

$$SIS(missing) = k_d \times SIS_{cloud-free}. \tag{6}$$

The cloud-free SISDNI was calculated as the ratio between the cloud-free direct irradiance and the cosine of the sun zenith angle θ.

After filling the gaps for missing values, we generated hourly and daily means of MSG data from instantaneous measurements taken every 15 min, while we aggregated hourly and daily averages of ground-based data from measurements taken at 1 min sampling interval. In both cases monthly means were produced from daily means, considering only those days in which both satellite and ground measurements were available. The procedure, generally adopted in literature, of comparing instantaneous satellite data with the synchronous 10 min averages of ground measurements, was not used in this paper, because the scope was to investigate if the model describes properly the variability of solar radiation at different time resolutions, rather than if it accurately reproduces ground measurements at the time of acquisition.

First we validated *all-sky* data. Then we split them according to three sky condition categories, namely *cloud-free*, *thin clouds* and *overcast*, and repeated the validation for each class. The discrimination was performed coherently with the cloud mask calculated with the method of Stöckli (2013), presented in the next subsection.

2.1. The method HelioMont for deriving SIS from MSG data

The algorithm implemented by MeteoSwiss for retrieving solar radiation from MSG data is presented in detail in Stöckli (2013) and shortly summarized here. Data from the SEVIRI (Spinning Enhanced Visible and Infrared Imager) instrument onboard the MSG satellites are used. This instrument has 12 channels in the visible and infrared bands for monitoring the reflected solar radiation and thermal emission of the Earth. SEVIRI has a spatial resolution at nadir of around 1 km for the high resolution visible channel and 3 km for the other channels.

The retrieval of the clear-sky global and direct beam irradiance is based on the GNU-MAGIC clear-sky model (Müller et al., 2009). RTM simulations with libRadtran (Mayer et al., 2005) are conducted for discrete values of aerosol optical properties, total column water vapor and ozone concentrations. The resulting look up tables are then applied to 6-hourly atmospheric states (water vapor and ozone) determined on the basis of numerical model output from ECMWF (Dee et al., 2011) and a monthly aerosol climatology (Kinne, 2009).

The cloud effect on clear-sky SIS is calculated by applying the well established HELIOSAT algorithm for dark surfaces, extended by a newly developed near-infrared and infrared cloud index for bright surfaces such as snow and desert. For identifying the state of each pixel MeteoSwiss adopts a probabilistic cloud mask based on the algorithm SPARC (Separation of Pixels using Aggregated Rating over Canada), proposed by Khlopenkov and Trishchenko (2007). The method was originally developed for AVHRR (Advanced Very High Resolution Radiometer) and adapted by MeteoSwiss to MSG SEVIRI (Fontana, Stöckli, & Wunderle, 2010). While most cloud masks use a classification tree, SPARC produces an additive rating from individual tests, which represents the probability of cloud contamination for each pixel. In addition to analyzing temperature, reflectance, and their spatial uniformity, two new tests are added to SPARC for testing the temporal variability of reflectance and temperature.

The surface radiation is finally calculated by scaling the expected clear-sky radiation with the clear-sky index (k), which is a function of the cloud index:

$$SIS = k(n) \times SIS_{cloud-free}. \tag{7}$$

MeteoSwiss has also implemented correction methods accounting for the effects of topography, such as shadowing, reflection, local horizon elevation angle and sky view factor. The Shuttle Radar Topography Mission (SRTM) digital elevation model, with a spatial resolution of 3 arc sec, is upscaled to 0.02° × 0.02° and used to determine the altitude and the horizon of each pixel.

2.2. Ground-based radiation data

We used three ground stations for the validation, two in the Swiss Alps and one in the Italian Alps (Fig. 1). All of the stations measure SIS, SISDIF and SISDNI.

The station of Bolzano (IT) is located at the valley floor, at an altitude of 262 MSL, at the junction of the three valleys: Val d'Isarco, Val Sarentina and Val d'Adige. The instruments are mounted at 1 m above ground, and in the surroundings there are the airport runway, crops and industrial facilities. In Bolzano observations are collected by three Kipp & Zonen instruments, i.e. 2 pyranometer model CMP11 (one measuring global irradiance and the other one combined with a sun tracker equipped with a shadow sphere that intercepts direct solar radiation for measuring diffuse radiation), and a pyrheliometer model CHP1 measuring direct irradiance. All the instruments used for the validation are regularly calibrated once per year.

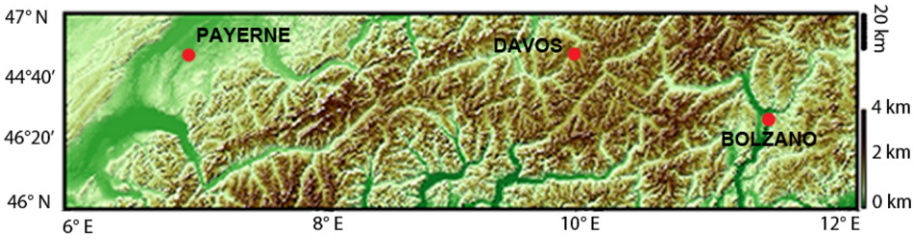

Fig. 1. Digital elevation model of the area of interest. Data from SRTM/NASA (Shuttle Radar Topography Mission) at 3 arc-second resolution. The red dots represent the measurement stations of solar radiation which we used in this study.

In Davos (CH) instruments are mounted at the Physical-Meteorological Observatory and World Radiation Center (PMO/WRC), at an altitude of 1610 MSL, on the wind mast of the Swiss Meteorological Institute, with grassland underneath. Data from Davos used in the present analysis were measured by two Kipp & Zonen CM21 pyranometers, one for global and the other for diffuse irradiance, and a Kipp & Zonen CHP1 pyrheliometer for direct normal irradiance. All the radiation instruments are mounted on an arm fixed at about 2 m distance from the main mast and about 4–8 m above the ground. The pyranometer measuring diffuse irradiance is equipped with a fixed shadow band pointing South.

The station of Payerne (CH) is part of the Baseline Surface Radiation Network (BSRN), which is a project of the Radiation Panel from the Global Energy and Water Cycle Experiment. The experiment aims at acquiring the best possible surface radiation budget information, and was initiated by the World Climate Research Programme. The radiation instruments of Payerne are located at MeteoSwiss, at an altitude of 491 MSL, and have grassland with crops in the vicinity. In Payerne direct normal irradiance is measured with a Kipp & Zonen CHP1, whereas global and diffuse irradiance are measured by two Kipp & Zonen CM21 pyranometers.

For this validation study we adopted 2011 as test year for performing the comparison between satellite and ground data in Bolzano and Davos, while in Payerne we carried out the analysis with data since 2004 to 2009, according to the availability of ground measurements.

2.3. Satellite and ground-based atmospheric data

In order to test the sensitivity of radiation components to atmospheric input, we also simulated solar radiation and its direct and diffuse components with the RTM libRadtran by using atmospheric inputs with a higher temporal resolution than the climatological ones used in the method of Stöckli (2013).

At the first stage, we took AERONET (AErosol RObotic NETwork) measurements of Aerosol Optical Thickness (AOT), Single Scattering Albedo (SSA), and precipitable water. AERONET is a global network of Sun Photometers (Holben et al., 1998). The sun photometer performs one direct measurement pointing at the sun, and one direct at the sky, at different wavelengths in the range 0.3–1.02 μm. This set of measurements allows a direct estimation of aerosol macro-physical properties such as AOT, and an indirect estimation of micro-physical properties, like the SSA. All the data from the sites around the world are collected and processed by NASA. Level 1.5 (cloud-screened) AOT, SSA and water vapor data for the stations of Bolzano and Davos have been downloaded from the AERONET website (http://aeronet.gsfc.nasa.gov).

At the second stage, considering the low number of AERONET stations in the Alps, for water vapor column amount we used the ERA Interim reanalysis of the ECMWF (European Centre for Medium-Range Weather Forecasts) at 0.25 × 0.25 degree grid, and for aerosol satellite data, specifically MODIS (MODerate resolution Imaging Spectroradiometer) retrieval of AOT, and OMI (Ozone Monitoring Instrument) SSA product. The instrument MODIS is on the EOS (Earth Observing System) Terra and Aqua polar orbiting satellites. It has 36 spectral bands between 0.41 and 14 μm. The satellites Terra and Aqua cross Europe at around 10:30 and 13:30 local solar time. MODIS AOT Collection 5 (Levy, Remer, Mattoo, Vermote, & Kaufman, 2007) over-land retrievals use four channels centered at 0.47, 0.66, 1.24 and 2.1 μm with a nominal resolution of 500 or 250 m at nadir. To reduce noise, the AOT at 0.55 μm is calculated in boxes of 10 × 10 km^2, averaging the 20 to 50 percentile of surface reflectance in each box. OMI is on EOS Aura polar orbiting satellites. Its measurements cover the spectral region between 264 and 504 nm, with a spectral resolution between 0.42 nm and 0.63 nm and a nominal ground footprint of 13 × 24 km^2 at nadir. Complete global coverage is achieved in one day.

3. Results

3.1. Validation of all-sky SIS, SISDIF and SISDNI

The results of the validation for the three stations of interest are summarized in Tables 1–3, respectively on the hourly, daily and monthly time scale, in terms of MAB and MBD, including both the all-sky and the specific sky conditions.

The validation of the monthly averages (Fig. 2(a)–(b)) indicates that the satellite estimation is useful to reproduce the seasonal cycle of the components of global radiation with a MAB of 3 W m^{-2} in flat terrain like Payerne and 7 and 12 W m^{-2} in steep terrain like Davos and Bolzano, respectively. Despite the agreement between the monthly averages of satellite and ground-based data, both in Bolzano and Davos diffuse irradiance is always overestimated by the satellite algorithm in the period of analysis (Table 3). This makes it interesting to investigate what happens on shorter time scales.

In Bolzano positive values of MBD were observed for all the irradiance components, both in the monthly, daily and hourly validation, suggesting that satellite data generally overestimate irradiance at this location. The local minimum of the monthly averages of SIS and SISDNI in June (Fig. 2(a)) is clearly associated with the low number of cloud-free days (only 2) and with the secondary peak of convective precipitations

Table 1
MAB and MBD (W m^{-2}) of the validation of hourly averages of global (GLO), diffuse (DIF) and direct normal (DNI) radiation for different sky conditions in Bolzano, Davos and Payerne.

Station	Years	Sky cond.	MAB [W m^{-2}]			MBD [W m^{-2}]		
			GLO	DIF	DNI	GLO	DIF	DNI
Bolzano (IT)	2011	All sky	52	40	128	6	15	−10
		Cloud-free	40	45	116	17	36	−24
		Thin clouds	51	31	121	4	−1	16
		Overcast	62	35	137	−17	−10	−18
Davos (CH)	2011	All sky	52	42	144	−6	14	−49
		Cloud-free	27	41	134	−5	38	−89
		Thin clouds	54	30	182	6	9	2
		Overcast	72	48	136	−12	−2	−45
Payerne (CH)	2004–2009	All sky	40	34	110	2	−5	22
		Cloud-free	20	30	96	10	12	−6
		Thin clouds	46	29	148	15	−13	73
		Overcast	49	38	89	−8	−11	17

Table 2
MAB and MBD (W m^{-2}) of the validation of daily averages of global (GLO), diffuse (DIF) and direct normal (DNI) radiation for different sky conditions in Bolzano, Davos and Payerne.

Station	Years	Sky cond.	MAB [W m^{-2}]			MBD [W m^{-2}]		
			GLO	DIF	DNI	GLO	DIF	DNI
Bolzano (IT)	2011	All sky	14	15	33	4	8	4
		Cloud-free	30	40	91	19	31	−5
		Thin clouds	46	30	115	1	−2	9
		Overcast	47	21	124	−20	−7	−31
Davos (CH)	2011	All sky	14	15	33	−2	7	−11
		Cloud-free	19	34	102	1	33	−70
		Thin clouds	49	24	162	7	4	22
		Overcast	51	29	102	−16	−2	−34
Payerne (CH)	2004–2009	All sky	10	11	31	1	−3	12
		Cloud-free	19	24	91	12	3	24
		Thin clouds	41	27	140	14	−13	74
		Overcast	32	25	70	−9	−12	16

which is typically observed in the Alps. The validation of the daily averages (Table 2) outlines difficulties in estimating diffuse irradiance from satellite data ($R^2 = 0.758$, MBD = 8 W m^{-2}, MAD = 15 W m^{-2}). Analogous results were observed for the hourly averages (Table 1) ($R^2 = 0.735$, MBD = 15 W m^{-2}, MAD = 40 W m^{-2}).

In Davos (Fig. 2(b)) the validation gives results similar to those recorded for Bolzano. A minimum of SIS and SISDNI is observed again in summer, and is associated with the high number of cloudy days (in June and July there were only 2 cloud-free days in total). Both monthly, daily and hourly analyses show that satellites overestimate diffuse irradiance (MBD >12%) and underestimate direct normal irradiance (MBD <−4%), although global irradiance turns out to be slightly underestimated in the hourly (MBD = −6 W m^{-2}) and daily (MBD = −2 W m^{-2}) analysis. Like for Bolzano, daily averages of diffuse irradiance are not as strongly correlated with ground data ($R^2 = 0.808$) as for global irradiance ($R^2 = 0.909$).

In Payerne (Fig. 2(c)) the validation shows high accuracy of the monthly-mean satellite global irradiance (MAB = 3 W m^{-2}, MBD = 1 W m^{-2}), and diffuse irradiance is only slightly underestimated (MBD = −3 W m^{-2}), whereas direct normal irradiance is overestimated (MBD = 14 W m^{-2}). The daily averages of the diffuse component over the 6 years of analysis are underestimated (MAB = −3 W m^{-2}) with $R^2 = 0.853$.

After having summarized the outcome of the analysis, it is important to clarify that the results obtained in Payerne are not climatologically equivalent to the ones obtained for the other two stations. The periods of investigation, in fact, have different lengths and do not overlap. In Bolzano and Davos we validated data of the year 2011 only, thus results are affected by the specific conditions of the year under investigation and are suitable for understanding if the satellite algorithm describes properly the short term variability of the irradiance components. On the other hand, results for Payerne were derived from the analysis of six years of data, consequently they can be considered representative for the long term pattern of the error in the satellite estimation of solar radiation.

Table 3
RMSE, MAB and MBD (W m^{-2}) for the monthly averages of global (GLO), diffuse (DIF) and direct normal (DNI) radiation in Bolzano, Davos and Payerne. The second row indicates for each station the same parameters in percentage of the corresponding mean value of ground measurements.

Station	GLO			DIF			DNI		
	RMSE	MAB	MBD	RMSE	MAB	MBD	RMSE	MAB	MBD
Bolzano	16	12	6	12	10	9	27	23	8
	6%	7%	4%	22%	1%	16%	14%	12%	4%
Davos	9	7	−1	9	7	7	18	13	−11
	5%	5%	0.2%	14%	14%	13%	9%	10%	−9%
Payerne	4	3	2	6	5	−3	21	18	14
	3%	2%	1%	9%	8%	−4%	15%	12%	10%

3.2. Validation of the mean diurnal cycle of SIS, SISDIF and SISDNI

In Bolzano and Davos the mean diurnal cycle (Fig. 3) reveals a strong overestimation of diffuse irradiance. Furthermore global irradiance is overestimated in the morning and underestimated during the rest of the day.

In Payerne the mean diurnal cycle (Fig. 4) shows a strong overestimation of direct normal irradiance, while diffuse irradiance is underestimated around noon, and global irradiance is overestimated in the morning and underestimated in the afternoon, similarly to the results observed for Bolzano and Davos.

The strong diurnal cycle of the estimation error is likely connected to the difference in spatial footprint of the data that we compared. A satellite pixel of 2 km^2 represents, in fact, the mean over substantial subgrid-scale topographic variability (slope, orientation, horizon altitude) and surface reflectance, whereas a station measurement is representative only for a small part of these topographic boundary conditions.

3.3. Validation of SIS, SISDIF and SISDNI under different sky conditions

In order to examine the most problematic conditions, we split data in classes according to the season and to the cloudiness status. Three cloudiness classes, i.e. cloud-free, thin clouds and overcast, were adopted, in accordance with the cloud mask computed by HelioMont. We considered an hour either cloud-free or overcast only if the cloud mask was equal to 0 or 2 respectively for all the time slots, while we classified an hour as thin clouds for mean hourly values of the cloud mask between 0.8 and 1.2. The remaining intermediate cases were excluded for avoiding mixing different sky conditions. For computing daily averages we selected only those hours in which both satellite and ground data belonging to a specific class were available.

The hourly (Table 1) and daily (Table 2) validation shows that in cloud-free conditions the estimation error of the irradiance components is much higher than in the other cases, especially in Bolzano and Davos, where diffuse radiation is strongly overestimated (MBD is in the range 31–38 W m^{-2}) and direct normal irradiance is underestimated up to 89 W m^{-2}. Considering these results, we calculated the monthly averages of diffuse radiation including only the time interval between 10 a.m. and 2 p.m., in order to quantify the influence on the yearly cycle of the estimation error considering only those hours in which most radiation is available (Fig. 5). In Bolzano and Davos MBD and MAB resulted much higher than under the other sky conditions, while in Payerne there was the opposite situation (see Table 4 for MBD and MAD values under thin clouds and overcast conditions). For direct normal radiation, MAD under cloud-free conditions was equal to 67, 103 and 55 W m^{-2} respectively in Bolzano, Davos and Payerne. In this case the error was comparable to the one observed under the other sky conditions.

In the next subsection we examine possible causes of error in the satellite estimation of diffuse radiation under clear-sky conditions.

3.4. Sources of error in the estimation of diffuse radiation

The behavior observed under clear-sky conditions can be partially explained considering processes and factors contributing to diffuse irradiance in the absence of clouds. They can be summarized as follows, together with a description of the model simplifications:

1. Mie scattering by aerosols is weakly wavelength selective, and particularly effective on visible light, where most of solar energy is concentrated: monthly values of aerosol optical characteristics are used to interpolate irradiance values from the look up tables. The

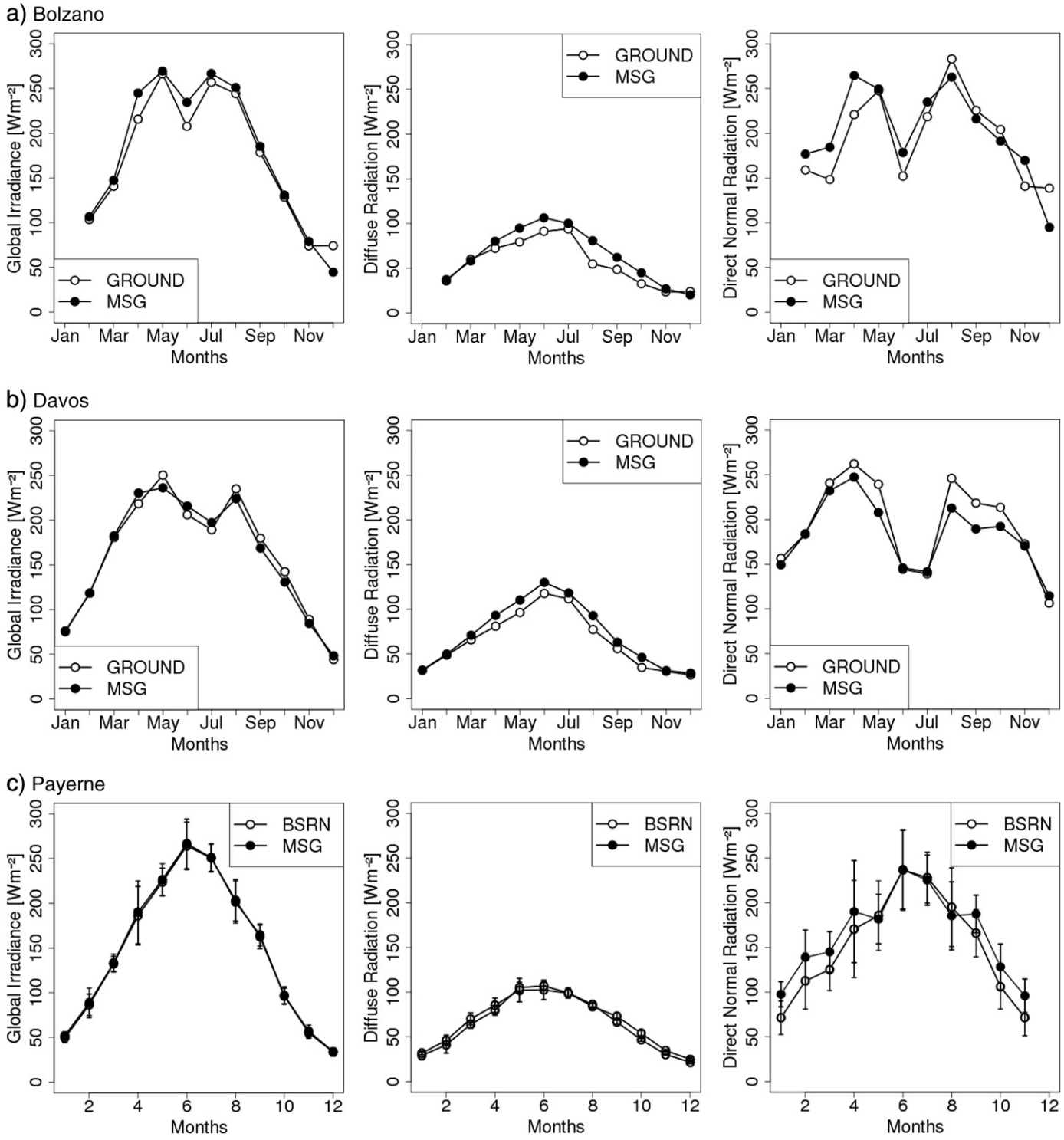

Fig. 2. Monthly averages of satellite and ground-based irradiance in Bolzano (2011), Davos (2011) and Payerne (2004 – 2009). The local minima of global and direct normal irradiance in June and July in Bolzano and Davos are due to the high percentage of cloudy days. In Bolzano no data were available for January because the radiometers were installed in February 2011. In panel (c) the error bars represent the inter-annual standard deviation of monthly averages of satellite and ground measurements. Given its low variability from year to year, the climatology of SISDIF can be considered representative of the single years.

global-scale 1° × 1° aerosol data cannot represent the vertical stratification of aerosols within the atmospheric boundary layer in complex topography. AOT at high elevation locations is thus likely to be overestimated by the satellite retrieval;

2. the global modeling approach of Kinne (2009) provides general information on amount, spatial distribution, and seasonality of aerosol properties at global scale, but is not representative for areas characterized by local complex orography. Both in Bolzano and Davos, in fact, the aerosol Kinne climatology adopted in Stöckli (2013) overestimates AOT, with a MBD of 0.1 in Davos (9 months of continuous measurements available), and 0.09 in Bolzano (only 3 and half months of measurements available) with respect to monthly averages of AERONET AOT in 2011. This causes the overestimation of diffuse radiation from satellite data;

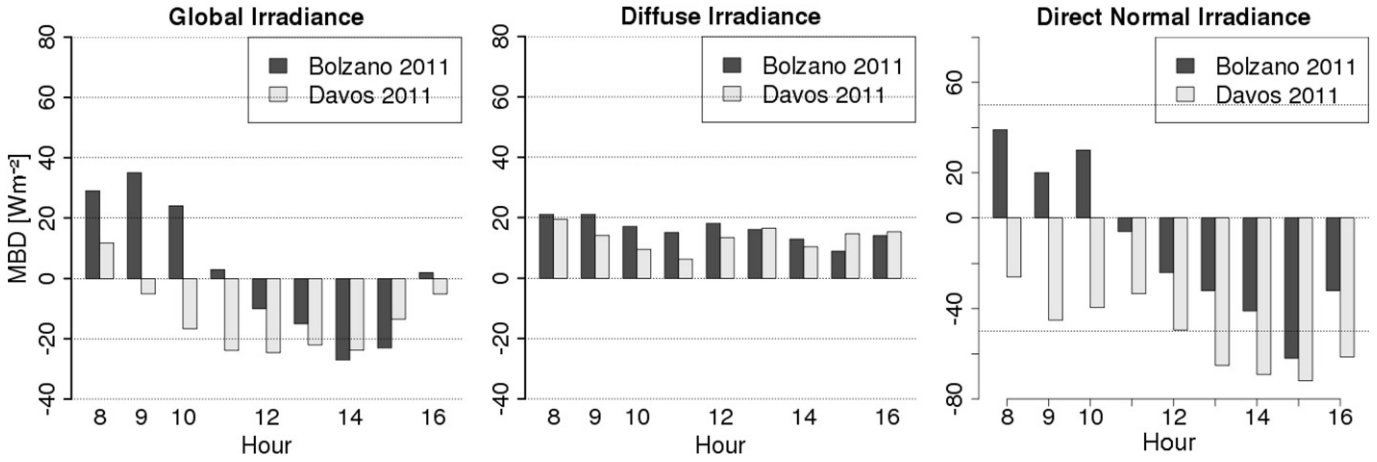

Fig. 3. Mean diurnal cycle of MBD of irradiance components in Bolzano and Davos. Only the data between 8 a.m. and 4 p.m. are represented because they are descriptive of the entire dataset, in fact in the remaining hours, during autumn and winter, the sun is below the local horizon.

3. Rayleigh scattering by atmospheric gases, whose effectiveness is confined in the ultraviolet part of solar spectrum, is much less relevant than Mie scattering on broadband radiation: the model assumes a fixed atmospheric profile (US standard atmosphere) and uses the *Kato band-parameterization* (Kato et al., 1999);
4. Surface reflection: the impact of surface albedo on clear-sky irradiance is approximated by using the clear-sky top-of-atmosphere reflectance as a surrogate for surface albedo. This approximation would need to be replaced by the estimation of an atmospherically corrected hemispherical surface albedo;
5. The sky-view-factor (see the next section for its definition) reduces diffuse radiation according to the visible portion of the sky vault: it is calculated from the horizon angle, thus is affected by the low resolution of the DEM, originally set at a resolution of 100 m, and then upscaled to the MSG high resolution visible channel pixel size, which is around 1 km East–West and around 1.7 km North–South. It is thus likely that the local-scale sky-view-factor at the valley stations Bolzano and Davos is lower compared to the sky view factor of the mean MSG high resolution visible channel pixel;
6. The diffuse-to-global ratio increases with optical air mass, i.e. with the sun zenith angle: this effect is considered by applying the *modified Lambert–Beer* relation, developed and validated in Müller et al. (2004) and EHF, UiB, and ARMINES (2003), and also verified in Ineichen (2006).

To summarize, the most critical approximations in the satellite-based clear-sky model are associated with aerosol scattering and surface reflectance. More in-depth examination is necessary for solving the surface-related issues. These problems have been partially addressed in Lee, Liou, and Hall (2011). In the next section we investigate the effects of aerosols and suggest a way to introduce more accurate data in the model.

4. Modeling the effect of aerosols

Since the validation study highlighted problems in the estimation of irradiance components under clear-sky conditions, it is interesting to quantify the influence of atmospheric absorption and scattering on direct and diffuse solar radiation. We carried out this study for Bolzano and Davos, which are equipped with a sun-photometer measuring aerosol optical properties and water vapor column amount, and are part of the AERONET network. The most interesting days to investigate would have been the summer days in which the largest discrepancy was observed. However data analysis had to be adapted to data availability, thus it was limited to the months containing most cloud-free days and for which most AERONET data were available, i.e. August for Bolzano and November for Davos.

We used AERONET measurements of AOT, SSA, and precipitable water. Then we calculated daily averages of these atmospheric parameters and

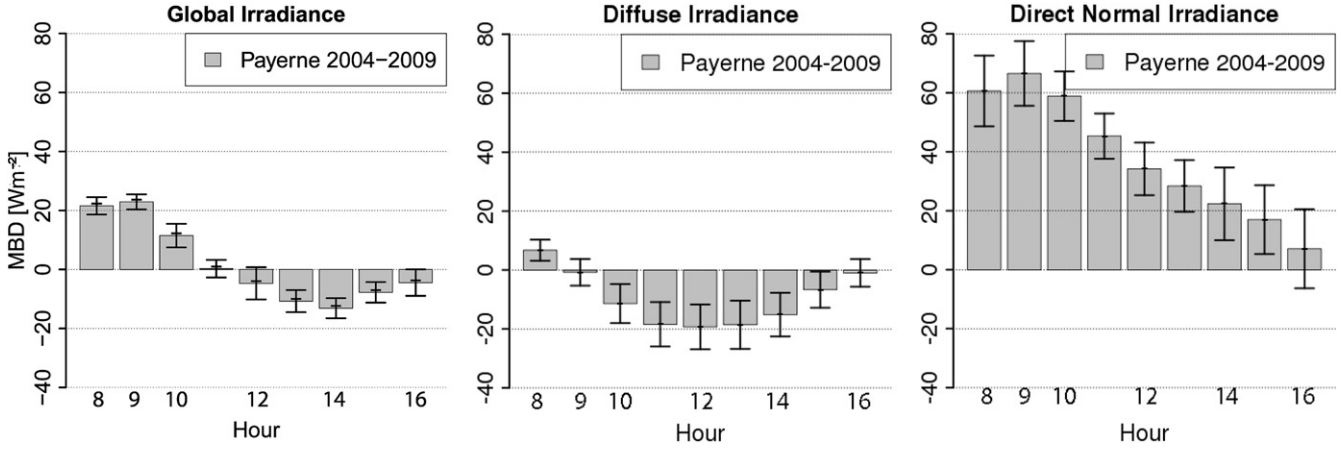

Fig. 4. Mean diurnal cycle of MBD of irradiance components in Payerne. Only the data between 8 a.m. and 4 p.m. are represented because they are descriptive of the entire dataset, in fact in the remaining hours, during autumn and winter, the sunis below the local horizon. The error bars represent the standard deviation of the daily cycle of MBD in the 6 years 2004—2009.

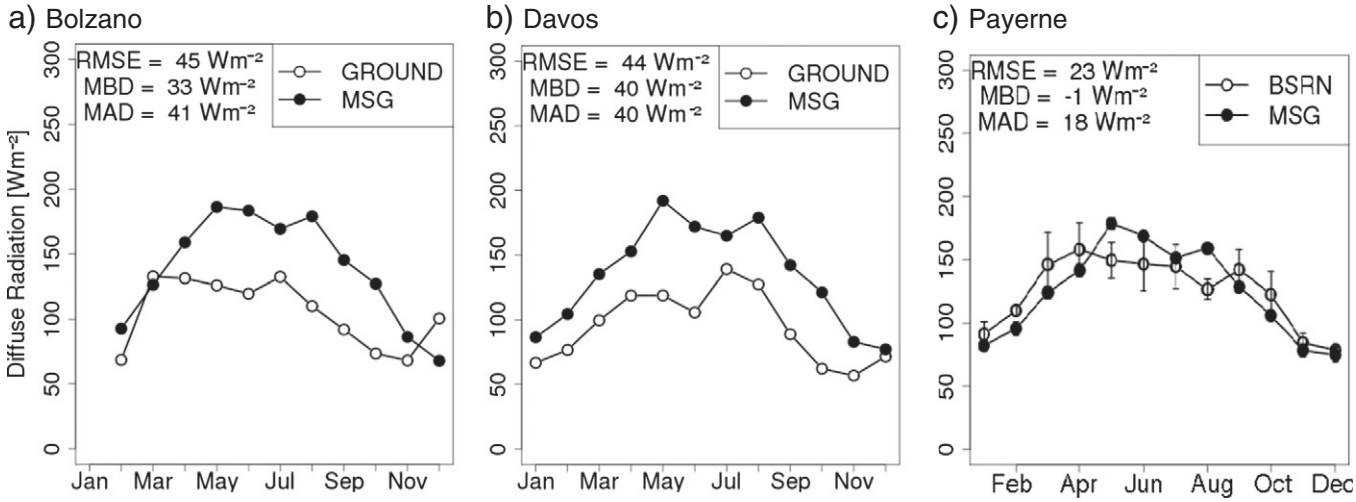

Fig. 5. Monthly averages of satellite and ground measurement of diffuse irradiance in Bolzano (2011), Davos (2011) and Payerne (2004−2009) under clear-sky conditions. Only the time interval between 10 a.m. and 2 p.m. was considered in the averaging of cloud mask and irradiance because in these hours most of the irradiance is available.

assumed them constant throughout each day in the simulations. The surface albedo was derived from the MODIS/Terra + Aqua Albedo 16-Day product (MCD43C3) with a resolution of 0.05°. Ozone column amount was set constant and equal to 300 Dobson units.

We modeled diffuse and direct radiation by the RTM libRadtran (Fig. 6), adopting as radiative transfer equation solver the discrete ordinate code *disort* (Stamnes et al., 1988) with 6 streams. The correlated-*k* approach of Kato et al. (1999) was used to compute the spectral transmittance assembling the absorption coefficients of different gases. We performed RTM runs every 15 min in the time interval between 10 a.m. and 2:45 p.m. in which the influence of shadowing is the smallest.

We reduced the simulated diffuse irradiance considering the sky view factor, f_s:

$$SISDIF_{cor} = SISDIF \times f_s + SISDIF \times \alpha(1-f_s) \quad (8)$$

where α is the surface albedo and f_s is the ratio between diffuse irradiance at a point and that on an unobstructed horizontal surface (Dozier & Marks, 1987) under the assumption of isotropic distribution of diffuse irradiance. The skyview factor was calculated for Bolzano and Davos from the horizon angle, and was equal, respectively, to 0.947 and 0.953.

As shown in Fig. 7(a) and (b), libRadtran simulates diffuse radiation with high accuracy when site-specific aerosol and water vapor measurements are used (MAB on hourly averages is 11 W m^{-2} in Bolzano and 5 W m^{-2} in Davos, MBD is 4 W m^{-2} in Bolzano and −5 W m^{-2} in Davos), while the satellite estimate significantly exceeds ground measurements in clear-sky days (MBD is 73 W m^{-2} in Bolzano and 32 W m^{-2} in Davos). Simulated direct irradiance is also very close to ground truth (MAB on hourly averages is 20 W m^{-2} in Bolzano and 10 W m^{-2} in Davos, MBD is 14 W m^{-2} in Bolzano and −4.5 W m^{-2} in Davos) compared to the satellite estimate (MAB is 83 W m^{-2} in Bolzano and 47 W m^{-2} in Davos). The latter result is significant, because direct irradiance is not sensitive to the effect of multiple scattering and surface albedo, and its inspection allows to better quantify the effect of aerosol absorption and single scattering.

Only four AERONET stations are based in the Alps at Davos, Bolzano, Laegern (47°.48 N, 8°.35 E, 735 m MSL) and Jungfrau (46°.55 N, 7°.98 E, 3580 m MSL). Consequently, in order to obtain spatially distributed information on aerosols, we used AOT from MODIS (10 km × 10 km), SSA from OMI (0.25° × 0.25°) and water vapor total column amount from the ERA Interim reanalysis of the ECMWF (0.25° × 0.25°).

Table 4
MAB and MBD (W m^{-2}) for the monthly averages of diffuse radiation in Bolzano (2011), Davos (2011) and Payerne (2004–2009) under thin clouds (TC) and overcast (OC) conditions. Only the time interval between 10 a.m. and 2 p.m. was considered in the averaging of cloud mask and irradiance because it was observed that most of the estimation error was concentrated in these hours, which are also those in which most of the irradiance is available.

	MBD [W m^{-2}]		MAD [W m^{-2}]	
	TC	OC	TC	OC
Bolzano	−9	−23	19	24
Davos	2	−14	38	22
Payerne	−21	−24	32	25

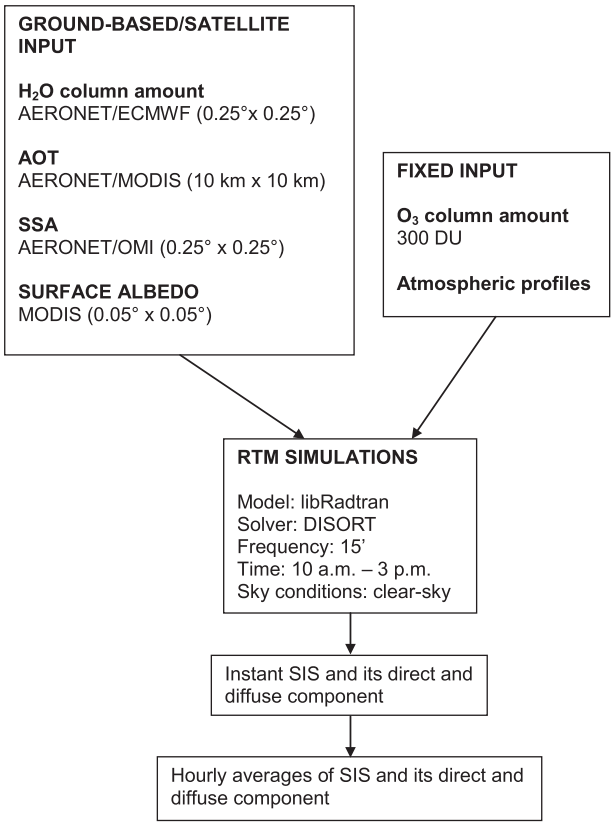

Fig. 6. Summary of the input used for performing RTM simulations in Bolzano and Davos.

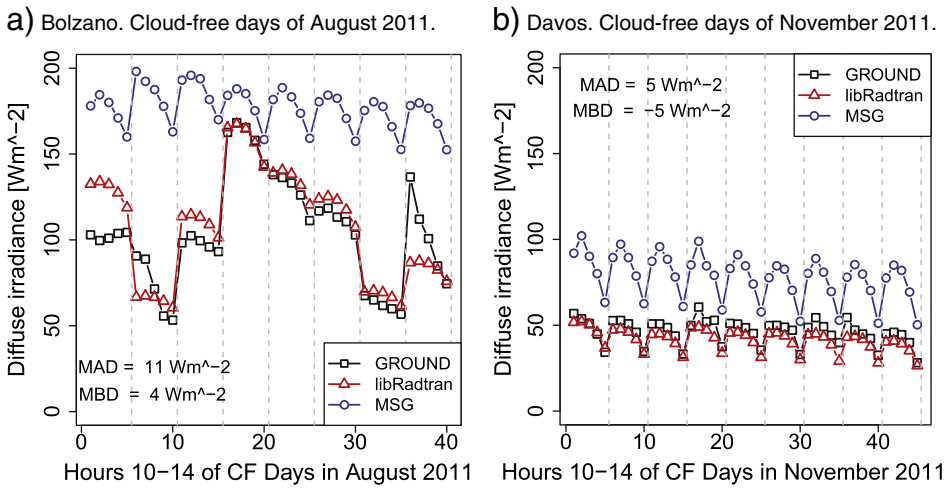

Fig. 7. Hourly averages of RTM simulations, ground measurements, and satellite retrieval of diffuse irradiance in Bolzano and Davos. MAD and MBD refer to the comparison between RTM simulations and ground measurements. Only the hours between 10 a.m. and 2 p.m. were considered. The daily averages of AOT, SSA and water vapor column amount measured by AERONET sun photometers were used as input for RTM simulations. The vertical dashed lines separate the days from each other. On the x axis there is the sequence cloud-free hours (40 for Bolzano, 45 for Davos) for which averages were computed.

In Bolzano we selected the clear-sky days of August 2011 in which MODIS data were available, and run simulations with the same settings as in the previous analysis. Finally we compared the hourly averages of simulated and ground-based data. The MAB of simulated diffuse irradiance against ground data resulted larger (27 W m^{-2}) than the one obtained by using AERONET data. Nevertheless results were much better than for the satellite estimation of diffuse radiation (MAB = 67 W m^{-2}). The same was observed for direct irradiance, in fact a MAB of 45 W m^{-2} was calculated, while for satellite data MAB was equal to 77 W m^{-2}.

These results suggest that an accurate satellite estimate of irradiance components requires at least daily data on the composition and optical properties of the atmosphere.

5. Conclusions

This study examined the performance of the HelioMont algorithm for estimating solar radiation from MSG data in complex terrain. The validation is based on ground-based measurements collected at three alpine sites, namely Bolzano, Davos and Payerne. The first two lie on a valley floor, and both are surrounded by a steep orography. The first is at low altitude, the second at high altitude. The third station is located on the Swiss Main Plateau. We analyzed the performance of the algorithm for different time scales, seasons and sky conditions in order to isolate specific drivers for the major remaining error sources.

The validation demonstrates that the algorithm is able to provide monthly climatologies of both global irradiance and its components over complex terrain. In addition the use of a cloud index based on the SEVIRI high resolution visible channel, as well as its subsequent extension with near-infrared and infrared channels over bright snow surfaces, provides a realistic radiative cloud forcing for the three sites of interest, as already shown by Stöckli (2013). However the estimation of the diffuse and direct components of irradiance on daily and hourly time scale is associated with considerable error. This problem is most prominent under clear-sky conditions, during summer-time, in the central hours of the day. In conclusion, the satellite algorithm overestimates atmospheric diffusivity, which in clear-sky conditions is mainly due to Mie scattering by aerosols and reflection by the Earth surface, and overestimates atmospheric absorption by aerosols and water vapor.

The clear-sky scheme of the satellite algorithm is driven with a monthly 1° × 1° climatology of aerosol distribution in the atmosphere. This external boundary condition offers a rather inadequate representation, both in spatial and in temporal resolution, of conditions occurring in Alpine valleys. To envisage how the estimation of the irradiance components can be improved, we used daily averages of accurate aerosol and water vapor data, available from the AERONET stations of Bolzano and Davos. For each station we selected the month with the highest number of cloud-free days and simulated the corresponding radiation by the RTM libRadtran, the same used in the satellite algorithm, also considering the sky view factor. Therefore we compared hourly averages of simulated, measured and estimated diffuse and direct irradiance. The low values of MBD and MAB between RTM simulations and ground measurements, compared to the high ones of satellite data, confirmed that model performance would benefit from more accurate local-scale aerosol boundary conditions.

AERONET stations provide very accurate information on aerosols, but are sparsely distributed all over the world. Consequently it is crucial to rely on other sources of data. The easiest choice is using satellite data. This option was tested in Bolzano running RTM simulations using MODIS AOT, OMI SSA and ERA Interim water vapor column amount. MAB duplicated compared to AERONET, but was still much lower than in satellite estimations. It can be concluded that despite having a reliable cloud forcing when deriving solar radiation from satellite data, there is room for improving such estimates by optimizing the prescribed atmospheric state under clear-sky conditions.

One option would be to use daily satellite-based aerosol maps. Known limitations of this method include the high retrieval errors of AOT over land with associated gaps in the dataset over regions with bright surfaces and cloud cover. Specifically non-vegetated mountainous regions with snow cover are often not sufficiently covered by satellite-based aerosol datasets. Nevertheless this choice is promising considering the availability of the new MODIS high resolution (1 km) AOT product obtained with the algorithm MAIAC (Multi-Angle Implementation of Atmospheric Correction) (Emili, Lyapustin, et al., 2011; Lyapustin, Wang, Laszlo, & Korkin, 2012). Another option could be that of integrating satellite and in-situ measurements (Emili, Popp, Wunderle, Zebisch, & Petitta, 2011) in order to reduce the uncertainty in satellite retrieval of AOT. Yet another promising approach are aerosol re-analysis projects like MACC (Inness et al., 2013) and GOCART (Chin, Rood, Lin, Müller, & Thompson, 2000; Chin et al., 2002), which assimilate satellite-based aerosol states, integrate them with known aerosol sources, and project their global distribution by use of atmospheric transport models.

6. Outlook

The proposed integration of surface aerosol measurements with satellite measurements enhances the applicability of satellite data and is more valuable than the analysis of single isolated stations or station networks (Grigiante, Mottes, Zardi, & De Franceschi, 2011). The resulting method improves the reliability and precision of solar radiation estimates over complex terrain, which is a key requirement for applications pertaining both to short-term weather forecasting, and to long-term climatological assessment of available radiation.

One example of such an application is the mitigation of one main weakness of technologies based on solar energy, like photovoltaic and concentrated solar power systems, i.e. the fluctuating nature of the solar resource and its poor predictability. An accurate solar radiation estimate is useful for solar energy assessments since it supports decision-making in both the private and public sector, e.g. in building solar atlases, defining suitable plant locations, calculating the return of the investments, and assessing the solar energy potential and the energetic scenario of a region.

Agriculture and forest management are other examples of fields where such valuable information is required. Furthermore in the mountains incoming shortwave radiation is also the main driver of a number of typical atmospheric boundary-layer processes (Rotach & Zardi, 2007), especially in connection with the development of thermally driven winds along the inclines and the valleys (Laiti, Zardi, de Franceschi, & Rampanelli, 2013a,b; Serafin & Zardi, 2010a,b, 2011). The latter are key factors for the assessment of air quality in mountain valleys, where pollutants may arise from the main traffic corridors (de Franceschi & Zardi, 2009), as well as from major plants, such as waste incinerators (Ragazzi, Tirler, Angelucci, Zardi, & Rada, 2013).

Acknowledgments

This work was partly supported by the EU ERDF (2-1a-97) funded project PV-Initiative and by the Interreg Italy-Switzerland project PV-Alps (27454223). The authors would like to thank EUMETSAT for providing SEVIRI data, MeteoSwiss for providing irradiance data calculated from SEVIRI, and in particular the Principal Investigator and Site Scientists of the BSRN station of Payerne for ensuring the high quality of the data, PMOD/WRC for providing ground-based radiation and for maintaining the AERONET station of Davos, the MODIS and OMI teams for providing aerosol data, and ECMWF for providing reanalysis data. CIMEL calibration was performed at the AERONET-EUROPE calibration center (GOA), supported by ACTRIS (European Union Seventh Framework Program (FP7/2007–2013) under grant agreement no. 262254.)

Appendix A. List of acronyms and symbols

α	surface albedo
AERONET	AErosol RObotic NETwork
AOT	Aerosol Optical Thickness
AVHRR	Advanced Very High Resolution Radiometer
BSRN	Baseline Surface Radiation Network
CM-SAF	Satellite Application Facility on Climate Monitoring
ECMWF	European Centre for Medium-range Weather Forecasts
EOS	Earth Observing System
f_s	sky view factor
k	clear-sky index
MAB	Mean Absolute Bias
MBD	Mean Bias Deviation
MODIS	MODerate resolution Imaging Spectroradiometer
MSG	Meteosat Second Generation
n	cloud index
OMI	Ozone Monitoring Instrument
PV	Photovoltaic
RMSE	Root Mean Square Error
R	linear regression coefficient
RTM	Radiative Transfer Model
SEVIRI	Spinning Enhanced Visible and Infrared Imager
SIS	Surface Incoming Shortwave Radiation
SISDIF	Surface Incoming Shortwave Radiation — Diffuse component
SISDNI	Surface Incoming Shortwave Radiation — Direct Normal Irradiance
SPARC	Separation of Pixels using Aggregated Rating over Canada
SSA	Single Scattering Albedo
θ	sun zenith angle
WMO	World Meteorological Organization

References

Barber, G., Hoertz, P., Lee, S. -H., Abrams, N., Mikulca, J., Mallouk, T., et al. (2011). Utilization of direct and diffuse sunlight in a dye-sensitized solar cell — Silicon photovoltaic hybrid concentrator system. *The Journal of Physical Chemistry Letters*, *2*, 581–585.

Betcke, J., Kuhlemann, R., Hammer, A., Drews, A., Lorenz, E., Girodo, M., et al. (2006). Final report of the HELIOSAT-3 project. *Technical report*.

Beyer, H., Costanzo, C., & Heinemann, D. (1996). Modifications of the Heliosat procedure for irradiance estimates from satellite images. *Solar Energy*, *56*, 207–212.

Bonan, G. B. (2002). *Ecological climatology: Concepts and applications*. Cambridge University Press.

Cano, D., Monget, J., Albuisson, M., Guillard, H., Regas, N., & Wald, L. (1986). A method for the determination of the global solar radiation from meteorological satellite data. *Solar Energy*, *37*, 31–39.

Carrer, D., Lafont, S., Roujean, J. -L., Calvet, J. -C., Meurey, C., Le Moigne, P., et al. (2012). Incoming solar and infrared radiation derived from METEOSAT: Impact on the modeled land water and energy budget over France. *Journal of Hydrometeorology*, *13*, 504–520.

Chin, M., Ginoux, P., Kinne, S., Torres, O., Holben, B., Duncan, B., et al. (2002). Tropospheric aerosol optical thickness from the GOCART model and comparisons with satellite and sun photometer measurements. *Journal of the Atmospheric Sciences*, *59*, 461–483.

Chin, M., Rood, R., Lin, S. -J., Müller, J. -F., & Thompson, A. (2000). Atmospheric sulfur cycle simulated in the global model GOCART — Model description and global properties. *Journal of Geophysical Research*, *105*, 24–671.

de Franceschi, M., & Zardi, D. (2009). Study of wintertime high pollution episodes during the Brenner-South ALPNAP measurement campaign. *Meteorology and Atmospheric Physics*, *237–250*.

Dee, D., Uppala, S., Simmons, A., Berrisford, P., Poli, P., Kobayashi, S., et al. (2011). The ERA-Interim reanalysis: Configuration and performance of the data assimilation system. *Quarterly Journal of the Royal Meteorological Society*, *137*, 553–597.

Dozier, J., & Marks, D. (1987). Snow mapping and classification from Landsat Thematic Mapper data. *Annals of Glaciology*, *9*, 97–103.

Dubayah, R. (1992). Estimating net solar radiation using Landsat Thematic Mapper and digital elevation data. *Water Resources Research*, *28*, 2469–2484.

Dubayah, R., & Paul, M. (1995). Topographic solar radiation models for GIS. *International Journal of Geographical Information Systems*, *9*, 405–419.

Dürr, B., & Zelenka, A. (2009). Deriving surface global irradiance over the alpine region from Meteosat Second Generation data by supplementing the HELIOSAT method. *International Journal of Remote Sensing*, *30*, 5821–5841.

Dürr, B., Zelenka, A., Müller, R., & Philipona, R. (2010). Verification of CM-SAF and MeteoSwiss satellite based retrievals of surface shortwave irradiance over the Alpine region. *International Journal of Remote Sensing*, *31*, 4179–4198.

EHF, UiB, & ARMINES (2003). Report of the Heliosat-3 software package for solar irradiance retrieval, all sky working version. Deliverable D8.1 and D8.2. *Technical report*.

Emili, E., Lyapustin, A., Wang, Y., Popp, C., Korkin, S., Zebisch, M., et al. (2011). High spatial resolution aerosol retrieval with MAIAC: Application to mountain regions. *Journal of Geophysical Research*, *116*. http://dx.doi.org/10.1029/2011JD016297.

Emili, E., Popp, C., Wunderle, S., Zebisch, M., & Petitta, M. (2011). Mapping particulate matter in alpine regions with satellite and ground-based measurements: An exploratory study for data assimilation. *Atmospheric Environment*, *45*, 4344–4353. http://dx.doi.org/10.1016/j.atmosenv.2011.05.051.

Fontana, F., Stöckli, R., & Wunderle, S. (2010). *SPARC: A new scene identification algorithm for MSG SEVIRI. Report on modifications and validation*. Visiting scientist report. EUMETSAT satellite application facility on climate monitoring.

Fontoynont, M., Dumortier, D., Hammer, A., Olseth, J., Skartveit, A., Ineichen, P., et al. (1997). *SATELLIGHT—Processing of METEOSAT data for the production of high quality daylight and solar radiation available on a world wide web internet server*. Mid-term progress report, jor3-ct90041 SoDa-5-2-4, CNRS-ENTPE.

Fontoynont, M., Dumortier, D., Heinemann, D., Hammer, A., Olseth, J., Skartveit, A., et al. (1998). SATELLIGHT — A www server which provides high quality daylight and solar radiation data for western and central Europe. *Proc. 9th Conference on Satellite Meteorology and Oceanography, Paris, France* (pp. 434–437).

Giovannini, L., Zardi, D., & de Franceschi, M. (2011). Analysis of the urban thermal fingerprint of the city of Trento in the Alps. *Journal of Applied Meteorology and Climatology*, *50*, 1145–1162.

Giovannini, L., Zardi, D., & de Franceschi, M. (2013). Characterization of the thermal structure inside an urban canyon: Field measurements and validation of a simple model. *Journal of Applied Meteorology and Climatology*, *52*, 64–81.

Giovannini, L., Zardi, D., de Franceschi, M., & Chen, F. (2014). Numerical simulations of boundary-layer processes and urban-induced alterations in an Alpine valley. *International Journal of Climatology*, *34*, 1111–1131. http://dx.doi.org/10.1002/joc.375.

Grigiante, M., Mottes, F., Zardi, D., & De Franceschi, M. (2011). Experimental solar radiation measurements and their effectiveness in setting up a real-sky irradiance model. *Renewable Energy*, *36*, 1–8.

Hammer, A., Heinemann, D., Hoyer, C., Kuhlemann, R., Lorenz, E., Müller, R., et al. (2003). Solar energy assessment using remote sensing technologies. *Remote Sensing of Environment*, *86*, 423–432.

Holben, B., Eck, T., Slutsker, I., Tanre, D., Buis, J., Setzer, A., et al. (1998). AERONET — A federated instrument network and data archive for aerosol characterization. *Remote Sensing of Environment*, *66*, 1–16.

Ineichen, P. (2006). Comparison of eight clear sky broadband models against 16 independent data banks. *Solar Energy*, *80*, 468–478.

Ineichen, P., Barroso, C., Geiger, B., Hollmann, R., Marsouin, A., & Mueller, R. (2009). Satellite application facilities irradiance products: Hourly time step comparison and validation over Europe. *International Journal of Remote Sensing*, *30*, 5549–5571.

Inness, A., Baier, F., Benedetti, A., Bouarar, I., Chabrillat, S., Clark, H., et al. (2013). The MACC reanalysis: An 8 yr data set of atmospheric composition. *Atmospheric Chemistry and Physics*, *13*, 4073–4109.

Journée, M., & Bertrand, C. (2010). Improving the spatio-temporal distribution of surface solar radiation data by merging ground and satellite measurements. *Remote Sensing of Environment*, *114*, 2692–2704.

Kasten, F., Dehne, K., Behr, H., & Bergholter, D. (1984). Spatial and temporal distribution of diffuse and direct solar radiation in Germany. *Research report N. 84*. German Federal Ministry of Research and Technology.

Kato, S., Ackerman, T., Mather, J., & Clothiaux, E. (1999). The k-distribution method and correlated-k approximation for a shortwave radiative transfer model. *Journal of Quantitative Spectroscopy and Radiative Transfer*, *62*, 109–121.

Khlopenkov, K., & Trishchenko, A. (2007). SPARC: New cloud, snow, and cloud shadow detection scheme for historical 1-km AVHHR data over Canada. *Journal of Atmospheric and Oceanic Technology*, *24*, 322–343.

Kinne, S. (2009). *Clouds in the perturbed climate system. Chapter climatologies of cloud related aerosols. Part 1: Particle number and size*. Cambridge, Mass: MIT Press.

Laiti, L., Zardi, D., de Franceschi, M., & Rampanelli, G. (2013a). Atmospheric boundary layer structures associated with the Ora del Garda wind in the Alps as revealed from airborne and surface measurements. *Atmospheric Research*, *132–133*, 473–489. http://dx.doi.org/10.1016/j.atmosres.2013.07.00 (URL: http://www.sciencedirect.com/science/article/pii/S016980951300197X).

Laiti, L., Zardi, D., de Franceschi, M., & Rampanelli, G. (2013b). Residual kriging analysis of airborne measurements: Application to the mapping of atmospheric boundary-layer thermal structures in a mountain valley. *Atmospheric Science Letters*, *2013*, 79–85.

Lee, W., Liou, K., & Hall, A. (2011). Parameterization of solar fluxes over mountain surfaces for application to climate models. *Journal of Geophysical Research*, *116*. http://dx.doi.org/10.1029/2010JD014722.

Levy, R., Remer, L., Mattoo, S., Vermote, E., & Kaufman, Y. (2007). Second-generation operational algorithm: Retrieval of aerosol properties over land from inversion of moderate resolution imaging spectroradiometer spectral reflectance. *Journal of Geophysical Research*, *112*. http://dx.doi.org/10.1029/2006JD007811.

Liou, K. (2002). *An introduction to atmospheric radiation*, *Vol. 84*, Academic Press.

Lyapustin, A., Wang, Y., Laszlo, I., & Korkin, S. (2012). Improved cloud and snow screening in MAIAC aerosol retrievals using spectral and spatial analysis. *Atmospheric Measurement Techniques*, *5*, 843–850.

Mayer, B., & Kylling, A. (2005). Technical note: The libRadtran software package for radiative transfer calculations: Description and examples of use. *Atmospheric Chemistry and Physics*, *5*, 1855–1877.

Müller, R., Dagestad, K., Ineichen, P., Schroedter-Homscheidt, M., Cros, S., Dumortier, D., et al. (2004). Rethinking satellite-based solar irradiance modelling: The SOLIS clear-sky module. *Remote Sensing of Environment*, *91*, 160–174.

Müller, R., Matsoukas, C., Gratzki, A., Behr, H., & Hollmann, R. (2009). The CM-SAF operational scheme for the satellite based retrieval of solar surface irradiance–A LUT based eigenvector hybrid approach. *Remote Sensing of Environment*, *113*, 1012–1024.

Ragazzi, M., Tirler, W., Angelucci, G., Zardi, D., & Rada, E. (2013). Management of atmospheric pollutants from waste incineration processes: The case of Bozen. *Waste Management & Research*, *31*, 235–240.

Remund, J., Wald, L., Lefvre, M., Ranchin, T., & Page, J. (2003). Worldwide Linke turbidity information. *Proceedings of ISES Solar World Congress 2003*, *Vol. 400*.

Rigollier, C., Lefèvre, M., & Wald, L. (2004). The method Heliosat-2 for deriving shortwave solar radiation from satellite images. *Solar Energy*, *77*, 159–169.

Rotach, M., & Zardi, D. (2007). On the boundary-layer structure over highly complex terrain: Key findings from MAP. *Quarterly Journal of the Royal Meteorological Society*, *133*, 937–948.

Sellers, P., Dickinson, R., Randall, D., Betts, A., Hall, F., Berry, J., et al. (1997). Modeling the exchanges of energy, water, and carbon between continents and the atmosphere. *Science*, *275*, 502–509.

Sellers, P., Randall, D., Collatz, G., Berry, J., Field, C., Dazlich, D., et al. (1996). A revised land surface parameterization (SiB2) for atmospheric GCMs. Part I: Model formulation. *Journal of Climate*, *9*, 676–705.

Serafin, S., & Zardi, D. (2010a). Daytime heat transfer processes related to slope flows and turbulent convection in an idealized mountain valley. *Journal of Atmospheric Science*, 3739–3756.

Serafin, S., & Zardi, D. (2010b). Structure of the atmospheric boundary layer in the vicinity of a developing upslope flow system: A numerical model study. *Journal of Atmospheric Science*, 1171–1185.

Serafin, S., & Zardi, D. (2011). Daytime development of the boundary layer over a plain and in a valley under fair weather conditions: A comparison by means of idealized numerical simulations. *Journal of Atmospheric Science*, 2128–2141.

Stamnes, K., Tsay, S., Jayaweera, K., Wiscombe, W., et al. (1988). Numerically stable algorithm for discrete-ordinate-method radiative transfer in multiple scattering and emitting layered media. *Applied Optics*, *27*, 2502–2509.

Stamnes, K., Tsay, S., Wiscombe, W., & Laszlo, I. (2000). *DISORT, a general-purpose Fortran program for discrete-ordinate-method radiative transfer in scattering and emitting layered media: Documentation of methodology*. Goddard Space Flight Center, NASA.

Stöckli, R. (2013). The HelioMont surface radiation processing. *Scientific report MeteoSwiss*, *93*, MeteoSwiss: Federal Office of Meteorology and Climatology (119 pp.).

Wilks, D. S. (2011). *Statistical methods in the atmospheric sciences volume 91 in the International Geophysisc Series*. Academic Press.

World Meteorological Organization, W. M. O. (2008). *Guide to meteorological instruments and methods of observation. N. 8* (7th ed.). World Meteorological Organization.